ACS Catalysis

Research Article

Cite This: ACS Catal. 2018, 8, 8513–8524

pubs.acs.org/acscatalysis

Sub-Monolayer Control of Mixed-Oxide Support Composition in Catalysts via Atomic Layer Deposition: Selective Hydrogenation of Cinnamaldehyde Promoted by (SiO_2-ALD)-Pt/Al_2O_3

Zhihuan Weng[‡] and Francisco Zaera*

Department of Chemistry and UCR Center for Catalysis, University of California, Riverside, California 92521, United States

ABSTRACT: Alumina-supported platinum catalysts have been modified with silicon oxide thin films grown using atomic layer deposition (ALD) in order to tune the acid–base and electronic properties of the oxide, and their performance has been tested for the hydrogenation of cinnamaldehyde. It was found that the silica layers greatly increase the stability of the platinum nanoparticles, preventing their sintering during high-temperature calcinations without affecting access to the metal surface in any significant way; the extent of CO adsorption, measured by infrared absorption spectroscopy was found to decrease by only one-third after 6 SiO_2 ALD cycles. Additional Brønsted and Lewis acid sites were created upon the deposition of submonolayer coverages of silicon oxide, as probed via pyridine adsorption. The addition of the silicon oxide thin films reduced the overall activity of these catalysts but also increased their selectivity toward the production of the unsaturated alcohol. In addition, both turnover frequencies (TOFs) and selectivities were found to increase initially with reaction time in most cases, presumably the result of catalyst conditioning by the reaction mixture. Those improvements were seen to be retained upon recycling of the catalysts. The best catalysts in term of selectivity (≥85% of cinnamyl alcohol production, in terms of TOFs) were obtained after 3 or 4 ALD cycles, which were estimated to deposit approximately half of a monolayer of SiO_2. Based on these results, it is proposed that the added strong Brønsted acid sites at mixed Si–O–Al positions, possibly in synergy with the metal surface, may be responsible for the relative enhancement in the hydrogenation of C=O bonds detected.

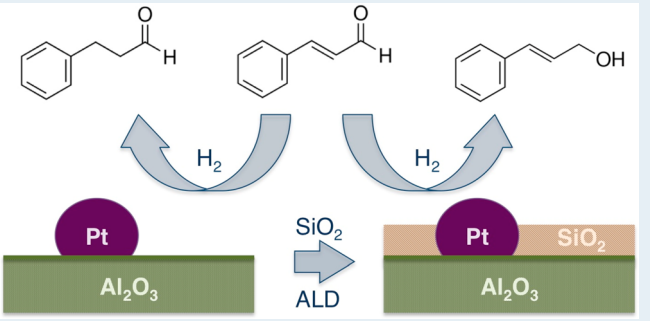

KEYWORDS: *atomic layer deposition, selective hydrogenation, platinum catalyst, unsaturated aldehydes, silica-alumina, infrared absorption spectroscopy, pyridine adsorption*

1. INTRODUCTION

In many heterogeneous catalysts the active phase, typically an expensive material such as a precious metal, is finely dispersed on a porous support in order to maximize its exposed surface.[1,2] In this scheme the support, often an oxide such as silica, alumina, titania, or ceria, has been traditionally viewed as inert, mainly providing the high surface areas needed for good dispersions of the main catalytic phase. Over the years, however, it has been shown that this is a simplistic picture and that the support itself does in most cases play an important role in defining the performance of catalysts. The chemistry of oxide supports has in fact being exploited in many processes, to take advantage of specific acid–base[3,4] or redox[5−7] sites within those solids, for instance. More recently, it has also become evident that new catalytic sites can be created at the interface between the support and the active phase, some with the ability to promote unique desirable reactions.[8,9] The controlled design and synthesis of those interfacial sites is still a challenge, however.

Atomic layer deposition (ALD) is a promising tool to tailor the properties of such interfaces. ALD is a chemical method for the deposition of thin solid films where monolayer control of the film thickness is attained by splitting the overall reactions into two or more complementary and self-limiting steps.[10−12] It is an approach popular in microelectronics and related applications[13−15] that is also finding its way into other fields of science and technology, including in catalysis.[16−21] Some reports are already available in the literature on the use of ALD to deposit and/or stabilize active catalytic phases such as metals on porous supports.[22−25] Less has been done to test its use for the modification of the support itself.[26−28]

Here we report data from a study on the use of ALD to modify the alumina surfaces of Pt/Al_2O_3 catalysts by depositing thin silica films. The hypothesis is that this way new mixed-oxide phases may form with unique catalytic properties. That idea was tested for the case of the selective hydrogenation of unsaturated aldehydes. It has been established that the support plays an important role in defining catalytic performance in those systems.[29−31] One consistent observation has been that the use of reducible oxides such as

Received: June 22, 2018
Revised: July 26, 2018

DOI: 10.1021/acscatal.8b02431
ACS Catal. 2018, 8, 8513–8524

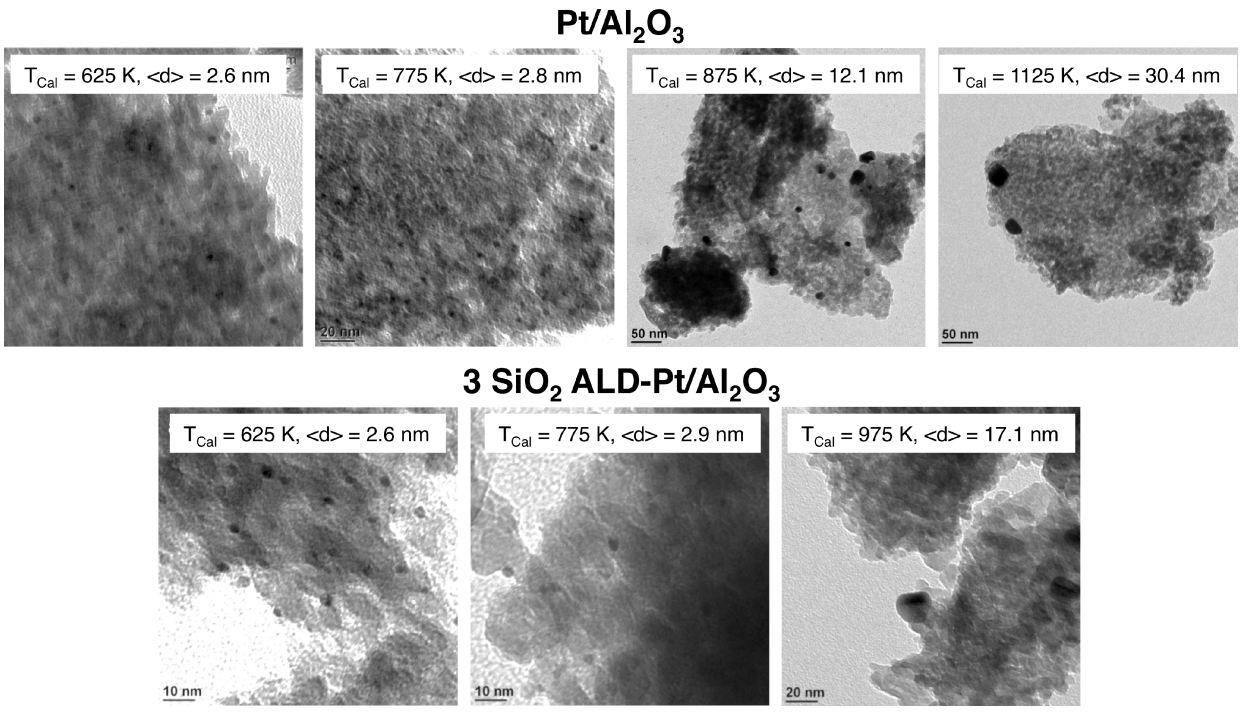

Figure 1. TEM images of Pt/Al_2O_3 catalysts, as obtained from the commercial supplier (top row) and after 3 SiO_2 ALD cycles (bottom row), as a function of calcination temperature. Sintering of the Pt nanoparticles is seen after calcination to temperatures above approximately 800 K, more extensively on the original catalyst.

titania or ceria leads to different, often better, performances than those seen with more conventional (silica or alumina) supports.[32−35] However, it is our contention that new sites with acid−base or redox properties may also be created in mixed oxides prepared using ALD, as already reported in a few cases.[36,37] Indeed, we found that the addition of thin silica layers to the alumina-supported catalyst significantly improves its selectivity toward the desired hydrogenation of C═O bonds, albeit at the expense of total activity. The new catalysts also proved to be more thermally stable. Our data provide an example of the power of ALD to tune the properties of oxide catalysts.

2. EXPERIMENTAL DETAILS

The initial Pt/Al_2O_3 catalyst used in these experiments was purchased from a commercial source (Sigma-Aldrich, 1 wt % metal loading). The silicon oxide ALD was performed by following a procedure inspired on a literature report,[38,39] following ALD chemistry well characterized by others.[40] The solid sample, placed in a small vial, was first suspended inside a round-bottom flask slightly above the surface of the liquid ALD precursor, tetramethyl orthosilicate (TMOS, Aldrich-Sigma, ≥99% purity), which was held at 355 K so that the solid sample could be exposed to the TMOS vapor. After 5 min of exposure to the TMOS, the vial with the powder was moved (under an inert atmosphere) to a two-neck flask, pumped for several minutes, and exposed to a mixture of water and ammonia vapors in a second round-bottom flask at room temperature for 10 min. The vial was transferred again to the two-neck-flask pumping stage to evacuate the water and ammonia vapors from the vial, and from there to the initial TMOS containing flask to initiate a new ALD cycle. This routine was repeated as many times as needed, as indicated in the individual reports of the data below. All catalysts were pretreated by reduction in a H_2 atmosphere at 625 K for 2 h prior to their use. The calcined samples were heated in air for 2 h at the temperatures indicated in the corresponding figures.

Carbon monoxide and pyridine adsorption on the resulting catalysts was characterized by infrared absorption spectroscopy in transmission mode, using a homemade quartz cell with NaCl windows and a Bruker Tensor 27 Fourier-transform infrared (FTIR) spectrometer.[41,42] The solids were pressed into pellet form, placed at the focal point of the sample compartment, and exposed to an atmosphere of the gas of interest, either carbon monoxide (Matheson Tri-Gas, ≥99.5% purity, 200 Torr, room temperature) or pyridine vapor (Sigma-Aldrich, ≥99.5% purity, ∼15 Torr, adsorbed at room temperature and then annealed at 425 K) for a fixed time (5−10 min) before pumping the volume of the cell and acquiring the IR data. The reported spectra correspond to averages of 512 scans taken at 4 cm^{-1} resolution and referenced to spectra for the catalyst before exposure. Transmission electron microscopy (TEM) images were obtained using a Philips Tecnai 12 instrument (120 kV accelerating voltage).

The kinetic measurements were performed using a 300 mL high-pressure Parr reactor following a procedure described in previous reports.[43] The catalyst (10 mg, 1.25 μmol Pt) and the cinnamaldehyde (Sigma-Aldrich, ≥95% purity; 82.5 mg, cinnamaldehyde/Pt mol ratio = 500:1) were mixed in 10 mL of isopropanol (Sigma-Aldrich, ≥99.7% purity, used as the solvent), and the reactor was pressurized with 30 bar of H_2 (Liquid Carbonic, >99.995% purity). The mixture was stirred continuously during the course of the reaction, which was carried out at room temperature (300 K). Aliquots of the reaction mixture were taken periodically using the sampling valve provided with the reactor (without opening the reactor) and analyzed by gas chromatography (HP50 Column 15 m ×

DOI: 10.1021/acscatal.8b02431
ACS Catal. 2018, 8, 8513−8524

0.32 mm × 0.25 μm, FID detection). The solid catalyst was filtered after reaction and washed with acetone for further analysis or for reuse in recycling experiments.

The original kinetic data are reported in terms of either percentage of conversion or turnover numbers (TONs) versus time; the latter corresponds to the number of cinnamaldehyde molecules converted per total number of Pt atoms in the catalyst. Assuming an average Pt particle size of 2.6 nm, as measured by TEM (Figure 1, left panels, for T_{calc} = 625 K), it is estimated that only about half of the Pt atoms of our catalysts are exposed on the surface of the nanoparticles, which means that the TON_{surf} expressed in terms of molecules converted per Pt surface atom would be approximately twice as large as those reported here. Because this is a systematic correction, however, it does not affect the calculations of reaction selectivities or any relative comparisons made in the discussion. Turnover frequencies (TOFs) were calculated by numerical differentiation of the TON-versus-time plots and are reported in units of TON/h.

3. RESULTS

3.1. Catalyst Characterization. Several catalysts were prepared by depositing silica thin films of various thicknesses on the starting Pt/Al_2O_3 commercial catalyst. Between 1 and 10 ALD cycles were used. Previous data from our laboratory for the ALD of SiO_2 films on mesoporous materials led to an estimation of the SiO_2 deposition rate of approximately 0.35 Å/cycle, which means that the films grown here on our Pt/Al_2O_3 catalysts range from 0.35 to 3.5 Å in thickness.[39] These layers were too thin to be clearly visible by TEM (also because of the negligible difference in contrast between alumina and silica) but did not appear to affect the Pt nanoparticle size distribution, which was estimated to center around 2.6 ± 0.2 nm (Figure 1, left images).

Access to the Pt surface in the catalysts treated with SiO_2 ALD was assessed by performing carbon monoxide titration experiments, using infrared absorption spectroscopy as the detection tool. The relevant data, with focus on the C−O stretching frequency region, are displayed in Figure 2. All traces are qualitatively similar, displaying a main peak around 2070 cm^{-1}, corresponding to CO adsorption on Pt atop sites (mainly on Pt(111) terraces), and a less intense and broader feature about ∼1840 cm^{-1} typically associated with bonding on bridged and/or defect sites (Figure 2, left panel).[44] The most significant result from these spectra is the reduction in peak intensity of the adsorbed CO features with increasing SiO_2 ALD cycles (Figure 2, right panel). Particularly noteworthy is the fact that such reduction is fairly limited: the atop CO signal intensity decreases only by about a third after 6 ALD cycles, which we estimate to correspond roughly to one SiO_2 monolayer. The size of the low-frequency peak due to bridge-bonded CO decreases in a more drastic fashion, losing about 3/4 of its intensity even after 3 cycles (as also seen in the past by other researchers),[45] but that is more difficult to interpret, as the bridge-bonded CO is more sensitive to structural or compositional changes on the surface. It is worth mentioning also that the frequency of the peak for atop CO, another parameter sensitive to the size and degree of exposure of the metal surface, remains the same (2070 cm^{-1}) for all the catalysts. The general conclusion deriving from the CO titration studies is that most of the Pt surface is still exposed and available for catalysis after the SiO_2 ALD treatments. It should be noted that previous reports have also shown that

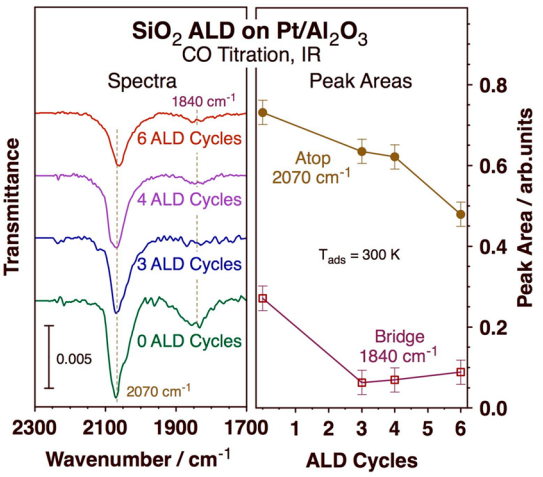

Figure 2. Left: Infrared absorption spectra for carbon monoxide adsorbed on Pt/Al_2O_3 catalysts treated with various (0, 3, 4, and 6) SiO_2 ALD cycles. Right: Peak intensities versus number of ALD cycles, estimated from the spectra on the left. Atop adsorption, manifested by the peak at 2070 cm^{-1}, is minimally suppressed by the growth of the silica layers.

oxide ALD on metal-supported catalysts does not fully block the metallic surface, in our case possibly because silica ALD occurs preferentially on oxide surfaces and is typically inhibited on metal substrates.[46] Also, it could be thought that the deposited silica films preferentially block specific facets of the metal nanoparticles, which could alter reaction selectivity; such structure-dependence has in fact been reported in the promotion of unsaturated aldehyde hydrogenation by Pt catalysts.[47] However, the reported nanoparticle-shape effects are small and could not account for the high selectivities for cinnamaldehyde hydrogenation at the C═O bond reported here (see below). Moreover, recent studies from our group have identified (111) terraces as the main sites for these reactions,[43] and, according to the CO IR titration data in Figure 2, those are only marginally blocked by the growing silica films.

Additional titrations experiments, with infrared absorption spectroscopy detection, were carried out using pyridine in order to characterize the different types of acid sites present on the surface and their evolution as the thickness of the ALD-deposited silicon oxide layer is increased.[48−50] The spectra recorded in those experiments are provided in Figure 3. The top trace, which corresponds to a Pt/SBA-15 sample added for reference, shows two main peaks at 1447 and 1595 cm^{-1} associated with hydrogen-bonded pyridine, as typically seen in silica-based catalysts.[51,52] The Pt/Al_2O_3 catalyst (bottom trace), by contrast, display several additional bands, at 1492, 1578, and 1614 cm^{-1}, from coordinately bonded pyridine on Lewis acidic sites, again in full agreement with previous reports.[51,52] The spectra from the samples modified by SiO_2-ALD (3 and 6 cycles) display most of the features of the original Pt/Al_2O_3 catalyst but also show some subtle differences indicative of a synergy between the aluminum oxide support and the silicon oxide thin films deposited on top. In particular, the peak at 1492 cm^{-1} grows in intensity, and two new features develop at 1547 and 1620 cm^{-1} (the latter seen as a shoulder of the 1614 cm^{-1} feature in the 6 ALD cycles sample). The first is typically associated with pyridinium ions, and is indicative of adsorption on strong Brønsted acid sites,

DOI: 10.1021/acscatal.8b02431
ACS Catal. 2018, 8, 8513−8524

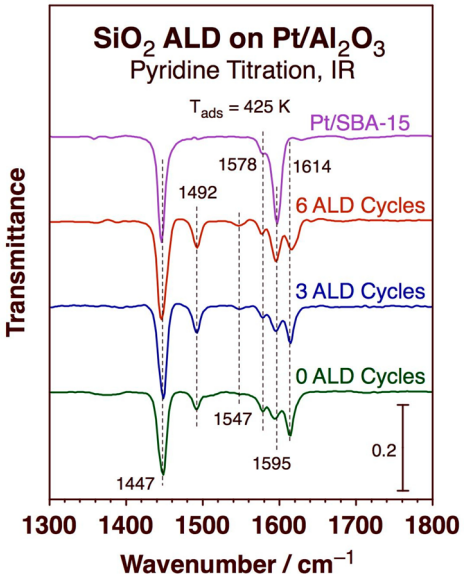

Figure 3. IR absorption spectra of pyridine adsorbed at 425 K on Pt/Al_2O_3 catalysts to which silicon oxide films of different thicknesses have been added via ALD (3 and 6 cycles). Data for Pt/Al_2O_3 and Pt/SBA-15 catalysts are also provided for reference. The new peaks that develop at 1547 and 1620 cm^{-1} indicate the creation of new strong Brønsted and Lewis sites on the mixed oxide surfaces.

whereas the latter has been ascribed to strong Lewis sites.[53] Note that although pure alumina itself does have Brønsted sites, adsorption on those has proven to be weak,[51] which means that the addition of silica on top must change their electronic configuration to make them more acidic. This type of synergy between the alumina original support and the silica overlayer to create new surface sites has been recently reported for dealuminated zeolites,[54] molecularly modified alumina,[55] and core−shell structures[56] as well.

3.2. Catalyst Activity and Selectivity. Next, the catalytic performance of our samples toward the hydrogenation of cinnamaldehyde (3-phenyl-prop-2-enal, CMA) was evaluated. The associated reactions are shown in Scheme 1. Figure 4

Scheme 1. Reaction Network Associated with the Initial Steps of the Hydrogenation of Cinnamaldehyde

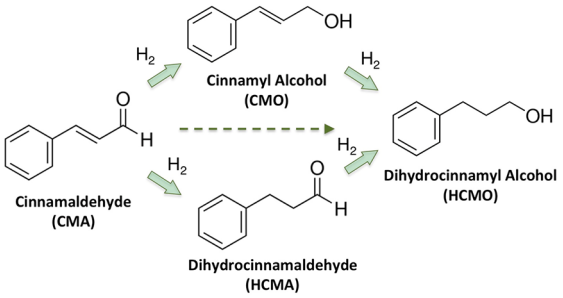

reports the time evolution of the total conversion (left panel) as well as the accumulation of cinnamyl alcohol (3-phenyl-prop-2-enol, CMO, second panel from left), dihydrocinnamaldehyde (3-phenyl-propanal, HCMA, third panel), and dihydrocinnamyl alcohol (3-phenyl-propanol, HCMO, right panel) versus reaction time in the batch reactor.

In terms of overall reactivity, Pt/Al_2O_3 proved to be the most active catalyst; close to 100% conversion could be achieved under our reaction conditions (cinnamaldehyde/Pt mole ratio = 500:1, P(H_2) = 30 bar, T = 300 K) in less than an hour. Similar high activities with alumina-supported platinum catalysts have been reported before.[57−59] However, the selectivity in this case is not high, since much HCMA and HCMO are produced together with the desired unsaturated alcohol (CMO) product. The addition of thin silicon oxide films to the original catalyst, via ALD, leads to a decrease in total activity but also to an increase in selectivity. The slowing down of the conversion is monotonic with increasing SiO_2 film thickness, until reaching a final slow performance after 6 ALD cycles; the reactivity data for 10 ALD cycles is similar to that obtained with the 6 ALD cycles sample.

Because the kinetic studies were carried out in a batch reactor, the raw data are presented in terms of TONs (or % conversion) versus time. To get a better sense of the time evolution of the reaction kinetics, those data were processed (differentiated) to estimate TOFs versus time. The results for the total CMO conversion are shown in Figure 5 as a function of both the time of reaction (left panel) and the percentage of conversion (right). These data show essentially the same trends reported in Figure 4 but also highlight an interesting additional observation, namely, that the reaction rates actually increase with time in the initial stages of the conversion, a trend opposite to what is typically seen in most other systems that suggests a degree of catalyst conditioning by the reaction mixture at the start of the reaction. This behavior is more pronounced in the alumina-based catalysts, in which case the TOF increases extend to very high conversions; upon the deposition of silica films on those catalysts, the performance approaches a more normal behavior, with the absolute rates of conversion decreasing with the extent of reaction. Again, those changes are accompanied by an overall decrease in catalytic activity with increasing silicon oxide film thickness.

Figure 6 reports the calculated selectivities toward the production of CMO in terms of TON versus reaction time (left panel) and % conversion (center) and of TOF versus % conversion (right). It is clearly seen in all these plots that the selectivities change significantly as the reaction proceeds. In addition, a dramatic increase in steady-state selectivity is seen upon the deposition of silicon oxide films on the Pt/Al_2O_3 catalyst, even after the addition of only a fraction of a SiO_2 monolayer: the final selectivity (estimated from the TON data, center panel), at high (>80%) conversions, jumps from approximately 25% with the original catalyst to over 60% with only 2 SiO_2 ALD cycles. It should be emphasized that, because of the slow rate of film growth in the SiO_2 ALD process, a 2-cycle treatment amounts to the deposition of a submonolayer coverage of the new oxide (an average thickness of ∼0.7 Å, which corresponds to between one-third and one-quarter of a monolayer based on the density of quartz). Therefore, the dramatic changes in selectivity reported here do not require much silicon oxide addition to the surface of the catalyst. Further increases in selectivity are seen upon the addition of thicker silica films, until an optimum value of close to 75% in terms of TONs (>85% in terms of TOFs) is reached with 4 SiO_2 ALD cycles. The addition of thicker films reverts this trend, and after 10 ALD cycles the maximum selectivity achieved goes back down to ∼60%.

A couple of additional interesting observations can be gleaned from the data in Figures 4−6. One is the fact that the initial evolution of the hydrogenation reaction that leads to increases in total TOFs (Figure 5) and selectivity (Figure 6)

DOI: 10.1021/acscatal.8b02431
ACS Catal. 2018, 8, 8513−8524

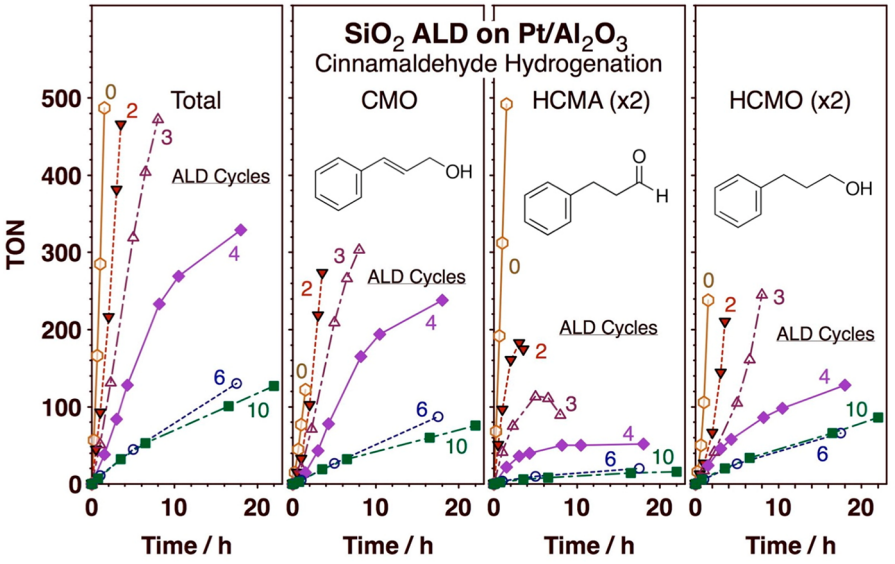

Figure 4. TONs versus time for the hydrogenation of cinnamaldehyde (CMA) on Pt/Al_2O_3 catalysts as a function of the number of ALD cycles used to deposit silicon oxide on the original solid. Shown are the data for the total conversion (left panel) as well as for the production of CMO (second panel), HCMA (third panel), and HCMO (last panel). The addition of silicon oxide films induces a decrease in total activity, the more the thicker the deposited film added, but also an increase in selectivity toward CMO.

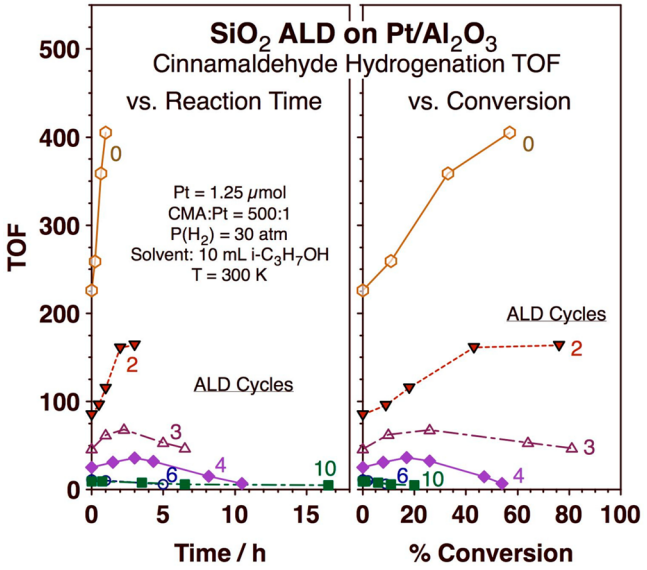

Figure 5. Total TOF versus reaction time (left panel) and versus % conversion (right panel) for the hydrogenation of cinnamaldehyde promoted with Pt/Al_2O_3 catalysts covered with silica films grown via ALD. The data, which were calculated by numerical differentiation of the original results in Figure 4, are provided for samples made with increasing number of ALD cycles, from 0 to 10. Interestingly, the TOFs increase with both reaction time and the extent of conversion in the initial stages of the reaction.

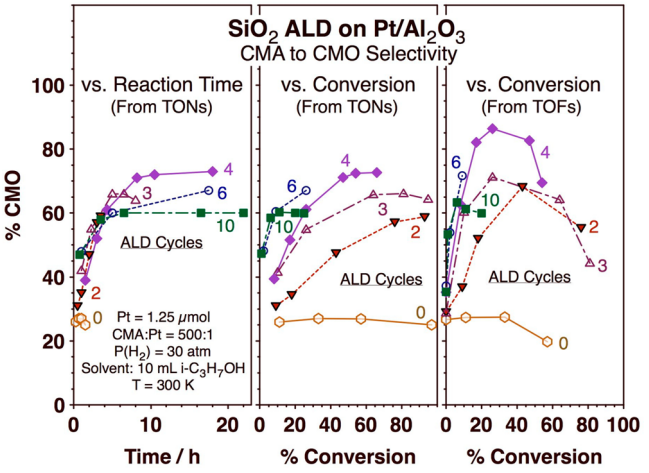

Figure 6. Selectivity toward CMO production, in terms of TONs versus time (left) and % conversion (center) and of TOFs versus % conversion (right), all as a function of the number of SiO_2 ALD cycles used in the making of the silica-modified Pt/Al_2O_3 catalysts. The steady-state selectivity (at high conversions) increases with silicon oxide film thickness until reaching a maximum at 4 SiO_2 ALD cycles, after which it decreases again.

occurs over a similar period of time, about 5 min, with all the catalysts regardless of the thickness of the silicon oxide film deposited. The effect is more clearly seen in the left panel of Figure 6, where the traces for the selectivity of the different catalysts lie on top of each other when plotted versus reaction time regardless of the extent of conversion (which varies as the total activity slows down with film thickness, as seen in the center and right panels of Figure 6). We speculate that perhaps some of the reactants (CMA) adsorb and get converted on specific sites within the surface of the catalyst, possibly on acid sites, to produce carbonaceous deposits, and that those temper the decomposition activity of the support and increase reaction selectivity. The end result is that more CMO is produced, in relative terms, than HCMA as the reaction progresses. It is particularly interesting to note that not only selectivity but also activity increases with time in this stage of the reaction. It has been shown that specific organic modifiers adsorbed on catalytic surfaces, self-assembled monolayers in particular, can lead to similar effects.[60−62]

The other observation worth pointing out is that selectivity toward CMO production decreases after long reaction times, that is, at high conversions. This is not surprising, since CMO can eventually be hydrogenated further to HCMO. What may be more informative is that such reaction appears to be slower

DOI: 10.1021/acscatal.8b02431
ACS Catal. 2018, 8, 8513−8524

than the conversion of HCMA to HCMO, so that the changes in selectivity due to variations in HCMO yields at high conversions are reflected mainly in the changes in HCMA yields (Figure 7). In fact, the net TOFs for HCMA reach

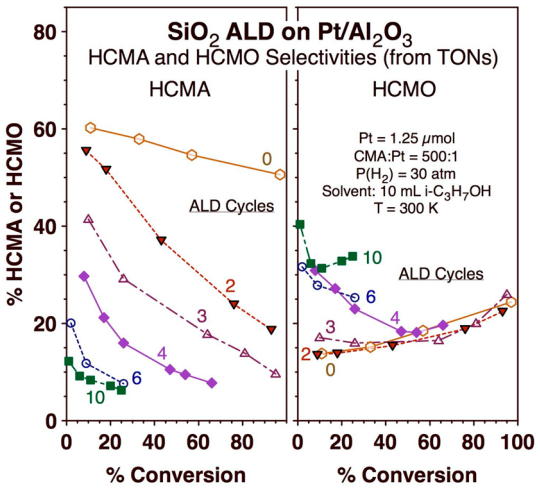

Figure 7. Selectivities for HCMA (left) and HCMO (right) production during the hydrogenation of cinnamaldehyde on Pt/Al_2O_3 as a function of the number of ALD cycles used to deposit silicon oxide on the surface of the catalyst. Less HCMA is made, in relative terms, as the reaction time increases in all cases, and less on the samples with the thicker silicon oxide layers. The production of HCMO is enhanced in relative terms by the addition of SiO_2 in the early stages of the reaction, but at high conversions the behavior is similar with all catalysts.

negative values in some cases (data not shown) as the rate of consumption of the HCMA (to produce HCMO) surpasses the rate of its production from CMA. In addition, there is an intrinsic rate of HCMO production that is detected even at the start of the catalytic runs. This indicates that HCMO is, to some extent at least, a primary product in this reaction. Although such early HCMO production is perhaps unexpected, it has been seen in some instances,[33,63] and recent molecular beam experiments on model platinum surfaces from our laboratory have proven that there can indeed be a direct path to full hydrogenation of the unsaturated aldehyde to the alcohol.[64] The fraction of HCMO produced in the initial stages of the catalysis increases with SiO_2 film thickness, up to a value of about 40% at $t = 0$ h with the 10 SiO_2 ALD sample, but then levels off with all catalysts, after about half of total conversion, to less than 20%. Because the large HCMO production is only seen at the start of the reaction, with the fresh catalysts, and because the effect is more pronounced with the silica-modified samples, we speculate that it may be related to the reactions at Brønsted acid sites that take place during the early catalyst conditioning, before reaching the steady-state performance.

3.3. Catalyst Stability. The observation that reaction rates go up with reaction time and the hypothesis that this may be due to preconditioning of the catalysts by the reaction mixture were explored further by performing recycling experiments. In these, the used catalyst was filtered from the solution after reaching 100% conversion of CMA in the initial mixture, washed with acetone, and treated in H_2 at 625 K for 2 h (but not calcined) prior to reuse. Figure 8 displays kinetic data obtained from such experiments for the cases of the original Pt/Al_2O_3 catalyst and a catalyst treated with 3 SiO_2 cycles, in

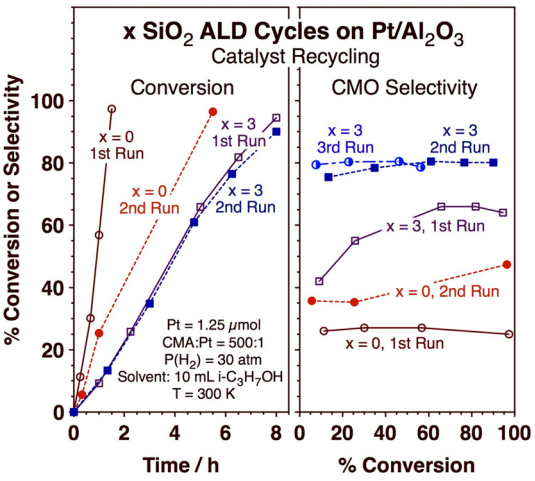

Figure 8. % Conversion versus reaction time (left) and CMO selectivity versus % conversion (right) for Pt/Al_2O_3 catalysts unmodified ($x = 0$) and after 3 SiO_2 ALD cycles ($x = 3$). Results are reported for sequential kinetic runs to test the recyclability of the catalysts. The reused catalysts display somewhat lower total activity but higher selectivities, especially in the case where the silica layer was added.

the form of total % conversion versus reaction time (left panel) and selectivity toward CMO production versus conversion. It was determined that while the original catalysts is partially poisoned and displays reduced activity in the second catalytic run, the one covered with a silica layer was more stable and retained its full activity the second time around (it showed a ~20% decrease in activity in the third run, data not shown). More critically, CMO selectivity increased over time and was retained in the used catalyst. With the pure Pt/Al_2O_3, additional increases were seen in the second run but to a final value around 40%. By contrast, the silica-treated catalyst reached a ~65% selectivity at the end of the first run and quickly stabilized at a final value of 80% by the end of the second run. It does appear that exposure of the catalysts to the reaction mixture modifies them in the initial stages of the conversion, in a process that leads to an increase in reaction selectivity. It should be mentioned that this evolution occurs without any changes in Pt particle size, as TEM images taken after reactions display the same size distributions as the pristine samples (data not shown).

The stability of the catalysts was also probed as a function of calcination temperature during their pretreatment. Calcination induces the sintering of the Pt nanoparticles, starting at temperatures above 800 K, as shown in the TEM images in Figure 1. This sintering, however, can be inhibited by the ALD of silicon oxide layers. Figure 9 shows TEM images that confirm this conclusion. Calcination at 975 K leads to significant increases in the average Pt particle size in the pure Pt/Al_2O_3 ($\langle d \rangle$ = 18.5 nm, images not shown) as well as in the catalyst treated with 3 SiO_2 ALD cycles but causes virtually no changes in the catalysts treated with either 6 or 10 SiO_2 ALD cycles. We estimate that 6 ALD cycles deposits the equivalent of one monolayer of silicon oxide on the surface.

The effect of these calcination pretreatments on catalytic performance is illustrated by the data in Figure 10 for the cases of the original catalyst and for the 3 ALD cycles sample. It is clear that high-temperature calcination results in a significant drop in total activity in both cases (left panel). The effect is

DOI: 10.1021/acscatal.8b02431
ACS Catal. 2018, 8, 8513−8524

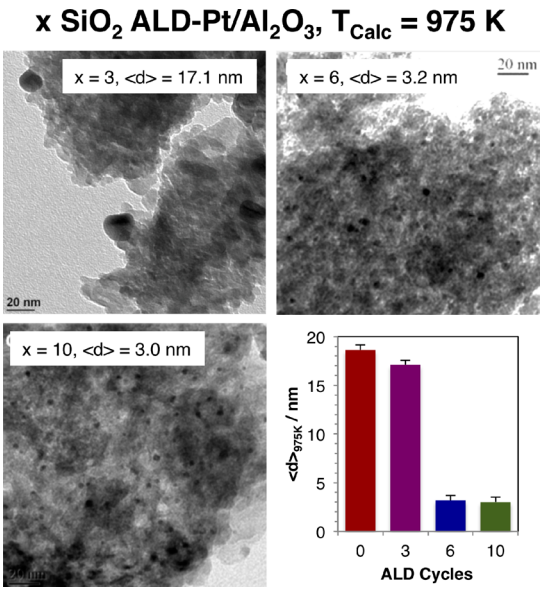

Figure 9. TEM images of Pt/Al_2O_3 catalysts obtained after 3 (top left), 6 (top right), and 10 (bottom left) SiO_2 ALD cycles followed by calcination at 975 K for 2 h. Bottom right: Average Pt particle size in the calcined samples as a function of ALD cycles. The added silica films are shown to prevent particle sintering.

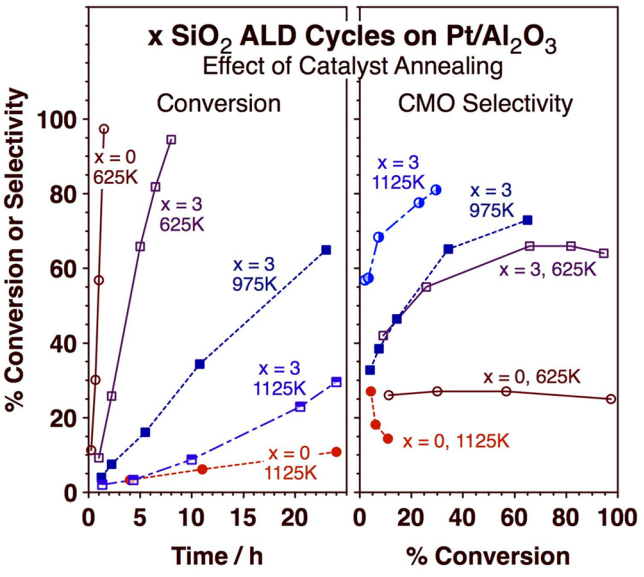

Figure 10. % Conversion versus reaction time (left) and CMO selectivity versus % conversion (right) for Pt/Al_2O_3 catalysts unmodified (x = 0) and after 3 SiO_2 ALD cycles (x = 3). Data are presented as a function of the temperature used for calcination during the catalyst pretreatment. Calcination at high temperatures results in a decrease in total activity in all cases. However, while selectivity increases in the catalyst with the silica layer, it decreases on the pure Pt/Al_2O_3 case.

more significant in the untreated alumina-based catalyst, presumably because sintering occurs to a greater extent there. Interestingly, the selectivity toward CMO production increases upon calcination in the 3 ALD sample but goes down with Pt/Al_2O_3 (right panel). There have been a few reports of selectivity changes in these reactions as a function of particle size, although the conclusions have differed across studies.[43,65,66] In our case, particle size may play a role, but the difference in trends between the catalysts with versus without added silica points to additional factors due to the support affecting catalytic performance as well.

4. DISCUSSION

The main purpose of this study has been to evaluate the feasibility of using ALD to tune the catalytic properties of oxides. Mixed oxides have been long used to systematically vary key properties such as acid−base or redox reactivity. This is particularly true with mixtures of aluminum and silicon oxides, in zeolites and other aluminosilicate compounds.[67−71] There, the substitution of silicon atoms with aluminum in the oxide network provides a way to add Lewis acid sites, and the change in the electron distribution to increase the Brønsted acidity in silanol groups adjacent to the new Al centers. Additional structures such as pentacoordinated or distorted tetrahedral Al may also be created this way.[67,72,73] However, in most cases, the mixed oxides are made as bulk solids, and that offers only limited flexibility in terms on tuning the properties of the surface. We here provide evidence that the acidity of alumina supports may be modified and their catalytic properties fine-tuned via the controlled addition of silicon oxide layers to their surfaces by ALD.[55]

The new catalysts reported by us were initiated from a standard alumina support, onto which platinum nanoparticles have been dispersed. This adds a new level of complexity, because much of the past work on the surface modification of oxide catalysts, of alumina in particular, has been carried out on the oxide alone. We show by CO site titration using infrared absorption spectroscopy that the addition of silica films to the Pt/Al_2O_3 catalysts does not significantly reduce the accessibility of gas molecules to the metal surface (Figure 2), possibly because the TMOS precursor in the silicon oxide ALD reacts preferentially on oxide sites. Ours seems to be a general observation, given that similar conclusions were reached by Feng et al. from studies on the coating of supported Pd catalysts with alumina films.[45,46] We also report the creation of new Brønsted and Lewis sites on the mixed oxide samples, as identified by pyridine titration and IR detection (Figure 3). The Brønsted sites become apparent by 3 ALD cycles, which we estimate leads to the deposition of approximately half a monolayer of silicon oxide, whereas the Lewis acid sites are more clearly seen after 6 ALD cycles, that is, after the completion of one SiO_2 monolayer. Because maximum reaction selectivity was seen with samples treated with 3 to 4 ALD cycles, we contend that it is the new Brønsted sites that may contribute to such selectivity optimization. As the selectivity peaks at one-half of a silica monolayer, the sites involved are most likely terminal silanol groups bonded to mixed Si−O−Al sites.

Some past spectroscopic studies have been directed at identifying the new sites generated by making mixed alumina-silica solids. However, the structure of those sites is still a matter of debate.[74] The accepted model, developed mainly in connection with hydrocarbon cracking catalysis, has been that the new Brønsted acidity arises from Al−OH groups close to silicon atoms.[75−77] Additional proposals have been put forward more recently, though, including acid sites with bridging Si−OH−Al groups[78−80] and silanol groups in the vicinity of aluminum atoms in different coordination configurations and oxidation states.[81,82] In all these cases, though, the studies have been based on bulk aluminosilicate samples.

DOI: 10.1021/acscatal.8b02431
ACS Catal. 2018, 8, 8513−8524

There are a few recent reports on the modification of alumina supports via the deposition of silicon-containing precursors. For instance, core−shell structures made by conformally coating Al_2O_3 nanospheres with SiO_2 films using sol−gel chemistry indicated that, if the silicon oxide film is thin enough (~2 nm), the underlying Lewis acidity of the alumina is quenched and replaced by strong Brønsted acid sites.[56] Using a gas-phase grafting procedure closely related to the ALD reported here, the group of van Bokhoven et al. showed that silica addition to alumina also yields Brønsted acid sites active for the dehydration of ethanol and the isomerization of *m*-xylene.[83,84] In a third example, Stair and co-workers modified γ-alumina samples with TEOS vapor and showed that the resulting monomeric SiO_x species on the alumina surface exhibit much higher specific activity than the parent alumina for the liquid-phase catalytic dehydration of cyclohexanol while retaining the same selectivity.[55] All these precedents are supportive of our idea that the silica ALD creates new strong Brønsted sites on mixed Si−O−Al sites. Note, however, that none of those catalyst included a metallic component, as is the case here. There are only a handful of precedents for the ALD or similar modification of surface of oxide supports in catalysts where the main active phase is a dispersed metal.[85]

Our central claim, deriving from this study, is that the formation of the new sites upon the addition of silica films to the alumina support, presumably the new strong mixed-oxide Brønsted acid sites, help increase the selectivity of the hydrogenation of unsaturated aldehydes toward the production of the corresponding unsaturated alcohols. Acid sites on solid supports are well-known to facilitate a number of skeletal rearrangements and bond-scission reactions in hydrocarbons and are used extensively in cracking and reforming processes.[86] Their role in selective hydrogenations, however, has been discussed to a much lesser extent. An early study reported that sonication of Pt/SiO_2 catalysts improves the selective hydrogenation of the C═O bonds (instead of the C═C moiety), an effect that the authors explained by claiming that sonication leads to the decoration of the metal nanoparticles with silica sites and that those favor the di-σ adsorption of the C═O fragment; this adsorbate is then proposed to interact with Si−OH acid sites to facilitate its hydrogenation.[87] There have also been indications that acid sites within the support of metal-based hydrogenation catalysts can promote more complex rearrangement reactions.[88,89] The fact that such reactions were not seen here suggests that promotion in our SiO_2-ALD-modified Pt/Al_2O_3 catalysts is the result of a synergy between the metallic and support sites (likely the new Brønsted acid sites in the later). Finally, it has been established that the use of reducible supports such as titania or ceria also enhances the selectivity of unsaturated aldehydes to unsaturated alcohols,[32,35,90−96] so the effect seen here with the silica-modified Pt/Al_2O_3 catalyst may be electronic, due to the creation of new unique sites at the metal-oxide interface.

Regarding the mechanism of the hydrogenation catalysis of unsaturated aldehydes using the new ALD-modified catalysts, our data may not afford sufficient information to put forward a detailed mechanism but do provide enough insights to extract a few general conclusions. First, as in many other catalytic hydrogenations, the role of the metal is critical, as virtually no conversion is seen without it. One of the main roles of the metal is to aid with H_2 activation to form adsorbed hydrogen atoms. Furthermore, the hydrogenation of unsaturated hydrocarbons, including unsaturated aldehydes, on metals is believed to take place stepwise, via the incorporation of one hydrogen atom at the time, via the so-called Horiuti-Polanyi mechanism.[29,97,98] Nevertheless, it is also clear that the nature of the support plays an important role in defining activity and selectivity for these reactions, since significant changes in catalytic performance were seen here as silica thin films were added to the starting Pt/Al_2O_3 material, and also given that others have reported different catalytic performance with different supports, as already mentioned above.

Not much discussion has been published about the direct effect of the properties of the support on unsaturated aldehyde hydrogenation reactions, but extensive knowledge is available on the role of the acidity of the support on related hydrocarbon reforming and cracking processes.[86] In those cases, the protonation of adsorbed surface species on Brønsted acid sites is believed to produce half-hydrogenated (ionic) intermediates analogous to those in the Horiuti-Polanyi mechanism on metals, which can then easily undergo further conversion, including not only full hydrogenation but also skeletal rearrangements and bond-scission and bond-forming steps. It is this protonation-initiated alternative mechanism that may be changing in our catalysts upon modification of the alumina support by the addition of silica. Extensive isomerization and cracking typically requires higher temperatures than those used here for the hydrogenation of cinnamaldehyde, but carbonaceous deposits from coupling of adsorbed carbon-containing species may still form on the support and potentially (selectively) poison some reaction sites on the Pt nanoparticles. The indication that this may be happening comes from our observation of changes in activity and selectivity versus reaction time (Figures 5−7) and upon recycling of the catalyst (Figure 8). It may seem odd that poisoning of the metal by strongly bonded carbonaceous deposits may lead to increases in absolute TOFs, as seen in the initial stages of our reactions (Figure 5), but those residues are an integral part of hydrogenation catalysis,[99] and similar rate increases has been reported in the past for the hydrogenation of related molecules such as furfural upon the addition of self-assembled monolayers on the surface.[62] More importantly, selectivity is easier to tune this way.

We finish with a brief discussion of the overall benefit of using ALD to modify the Pt catalysts for the hydrogenation of unsaturated aldehydes. Typically, selective catalysts are highly desirable because they use less reactants, produce less (potentially polluting) byproducts, and minimize the need for extra separation and purification steps.[100−102] However, improved selectivities often come at the expense of total activity, and a balance needs to be reached between these two conflicting criteria. That is the case here. However, the situation is not as dire as it may appear at first sight, because the gains in selectivity we report lead to a reduction in the difference in specific activity toward the desired products between the pure Pt/Al_2O_3 and SiO_2-ALD modified catalysts (compare to the differences in total activity). For instance, the maximum total TOF is about 400 TON/h for the alumina-only catalyst but only around 70 TON/h for the 3-SiO_2-ALD sample (Figure 5). On the other hand, the maximum TOFs for CMO production are 100 and 50 TON/h, respectively (calculated by combining the data from Figures 5 and 6). In fact, it is 110 TON/h with the 2-SiO_2-ALD sample (higher than with Pt/Al_2O_3)! Looking at the performance of the operational catalyst, after recycling (Figure 8), the picture is

DOI: 10.1021/acscatal.8b02431
ACS Catal. 2018, 8, 8513−8524

even more encouraging: the Pt/Al_2O_3 catalyst reaches steady-state total and CMO TOFs of ~100 and 40 TON/h, respectively, whereas for the 3-SiO_2-ALD sample the numbers are 40 and 32 TON/h, respectively. In other words, our silica-modified catalyst shows approximately 80% of the activity of the alumina supported catalysts as far as CMO production is concerned while avoiding the waste of the 60% of the reactant that would be converted to other undesirable products with the unmodified catalysts. The added catalyst stability shown by the data in Figure 9 is a bonus. In this light, we believe that the benefits of the ALD modification of the catalyst are clear.

5. CONCLUSIONS

The ability to control the chemical properties of oxide supports via their modification using ALD was tested for the specific case of the addition of SiO_2 films to Pt/Al_2O_3 catalysts. Several catalysts were prepared by carrying out between 0 and 10 SiO_2 ALD cycles, which were estimated to correspond to films thicknesses of up to approximately 2 monolayers. Infrared absorption spectroscopy characterization of the uptake of carbon monoxide on these catalysts led to the conclusion that adsorption on Pt atop sites is only suppressed by about a third after 6 ALD cycles (1 SiO_2 monolayer). The Pt bridge sites, on the other hand, were blocked after fewer ALD cycles and to a larger extent. The adsorption of pyridine uncovered the formation of new strong Brønsted and Lewis acid sites, manifested by new peaks in the infrared spectra at 1547 and 1620 cm^{-1}, respectively.

The silicon oxide films were found to reduce the ability of the Pt/Al_2O_3 catalysts to promote the hydrogenation of cinnamaldehyde but also to greatly increase their selectivity toward the unsaturated alcohol. The initial TOF decreased from over 200 h^{-1} with the unmodified catalyst to about 50 h^{-1} with the sample treated with 3 SiO_2-ALD cycles, to ~25 h^{-1} after 4 SiO_2-ALD cycles, and to ~10 h^{-1} after 6 SiO_2-ALD cycles. The latter correspond to one SiO_2 monolayer, and further silicon oxide addition did not lead to any additional changes in catalyst performance. Interestingly, the activity (and selectivity) of these catalysts increased during the initial stages of the reaction, presumably because of the in situ conditioning of the catalyst by the reaction mixture; those gains in catalytic performance were preserved upon the recycling of the catalysts and their reuse for the conversion of fresh reaction mixtures.

In terms of selectivity, the original Pt/Al_2O_3 catalyst was determined to only convert about 25−30% of the unsaturated aldehyde to the unsaturated alcohol, the desired product. However, addition of even small amounts of silica (as little as 2 ALD cycles) leads to an increase in maximum selectivity, to values above 60%. That selectivity does go down after high conversions because of further hydrogenation to the saturated alcohol, although the preferred route for that product is via the saturated aldehyde. Direct hydrogenation of about 10% of the unsaturated aldehyde (cinnamaldehyde) to the saturated alcohol (dihydrocinnamyl alcohol) was also seen, even in the initial stages of the conversion. The best performance in terms of selectivity was seen with the catalysts treated with 4 SiO_2-ALD cycles (leading to the growth of approximately one-half of a SiO_2 monolayer), in which case approximately 85% of the reactant could be converted to cinnamyl alcohol.

Finally, the thermal stability of these catalysts toward sintering was assessed. Both the original catalyst and samples modified with thin (≤3 ALD cycles) silicon oxide layers were found to sinter upon calcination at temperatures above ~800 K, as shown by significant increases in average particle sizes in TEM images. This sintering, however, was suppressed in the catalysts treated with either 6 or 10 SiO_2 ALD cycles: average Pt nanoparticle sizes of 3.0 ± 0.2 nm were measured after calcination of those samples in air at 975 K for 2 h, almost the same value, within experimental errors, of the original Pt/Al_2O_3 sample. The calcined catalysts displayed reduced activity but also noticeable improvements in selectivity.

AUTHOR INFORMATION

Corresponding Author

*E-mail: zaera@ucr.edu.

ORCID

Francisco Zaera: 0000-0002-0128-7221

Present Address

‡Z.W.: Department of Polymer Science & Engineering, Dalian University of Technology, Dalian 116024, People's Republic of China.

Notes

The authors declare no competing financial interest.

ACKNOWLEDGMENTS

Financial support for this project was provided by a grant from the U.S. National Science Foundation, Division of Chemistry, under Award No. NSF-1660433.

REFERENCES

(1) Thomas, J. M.; Thomas, W. J. *Introduction to the Principles of Heterogeneous Catalysis*; Academic Press: London, 1967.

(2) Ma, Z.; Zaera, F. Heterogeneous Catalysis by Metals. In *Encyclopedia of Inorganic and Bioinorganic Chemistry*; Scott, R. A., Ed.; John Wiley & Sons, Ltd: Chichester, U.K., 2014; p eibc0079.

(3) Corma, A. Inorganic Solid Acids and Their Use in Acid-Catalyzed Hydrocarbon Reactions. *Chem. Rev.* **1995**, *95*, 559−614.

(4) Pastore, H. O.; Coluccia, S.; Marchese, L. Porous Aluminophosphates: From Molecular Sieves to Designed Acid Catalysts. *Annu. Rev. Mater. Res.* **2005**, *35*, 351−395.

(5) Fujishima, A.; Zhang, X.; Tryk, D. A. TiO_2 Photocatalysis and Related Surface Phenomena. *Surf. Sci. Rep.* **2008**, *63*, 515−582.

(6) Vivier, L.; Duprez, D. Ceria-Based Solid Catalysts for Organic Chemistry. *ChemSusChem* **2010**, *3*, 654−678.

(7) Zhu, H.; Zhang, P.; Dai, S. Recent Advances of Lanthanum-Based Perovskite Oxides for Catalysis. *ACS Catal.* **2015**, *5*, 6370−6385.

(8) Green, I. X.; Tang, W.; Neurock, M.; Yates, J. T., Jr Spectroscopic Observation of Dual Catalytic Sites During Oxidation of CO on a Au/TiO_2 Catalyst. *Science* **2011**, *333*, 736−739.

(9) Rodriguez, J. A.; Senanayake, S. D.; Stacchiola, D.; Liu, P.; Hrbek, J. The Activation of Gold and the Water−Gas Shift Reaction: Insights from Studies with Model Catalysts. *Acc. Chem. Res.* **2014**, *47*, 773−782.

(10) George, S. M. Atomic Layer Deposition: An Overview. *Chem. Rev.* **2010**, *110*, 111−131.

(11) Zaera, F. The Surface Chemistry of Atomic Layer Depositions of Solid Thin Films. *J. Phys. Chem. Lett.* **2012**, *3*, 1301−1309.

(12) Knapas, K.; Ritala, M. In Situ Studies on Reaction Mechanisms in Atomic Layer Deposition. *Crit. Rev. Solid State Mater. Sci.* **2013**, *38*, 167−202.

(13) Zaera, F. The Surface Chemistry of Thin Film Atomic Layer Deposition (ALD) Processes for Electronic Device Manufacturing. *J. Mater. Chem.* **2008**, *18*, 3521−3526.

(14) Levitin, G.; Hess, D. W. Surface Reactions in Microelectronics Process Technology. *Annu. Rev. Chem. Biomol. Eng.* **2011**, *2*, 299−324.

DOI: 10.1021/acscatal.8b02431
ACS Catal. 2018, 8, 8513−8524

(15) Parsons, G. N.; Elam, J. W.; George, S. M.; Haukka, S.; Jeon, H.; Kessels, W. M. M.; Leskelä, M.; Poodt, P.; Ritala, M.; Rossnagel, S. M. History of Atomic Layer Deposition and Its Relationship with the American Vacuum Society. *J. Vac. Sci. Technol., A* **2013**, *31*, 050818.
(16) Zaera, F. New Challenges in Heterogeneous Catalysis for the 21st Century. *Catal. Lett.* **2012**, *142*, 501−516.
(17) Zaera, F. Nanostructured Materials for Applications in Heterogeneous Catalysis. *Chem. Soc. Rev.* **2013**, *42*, 2746−2762.
(18) O'Neill, B. J.; Jackson, D. H. K.; Lee, J.; Canlas, C.; Stair, P. C.; Marshall, C. L.; Elam, J. W.; Kuech, T. F.; Dumesic, J. A.; Huber, G. W. Catalyst Design with Atomic Layer Deposition. *ACS Catal.* **2015**, *5*, 1804−1825.
(19) Lu, J.; Elam, J. W.; Stair, P. C. Atomic Layer Deposition—Sequential Self-Limiting Surface Reactions for Advanced Catalyst "Bottom-up" Synthesis. *Surf. Sci. Rep.* **2016**, *71*, 410−472.
(20) Singh, J. A.; Yang, N.; Bent, S. F. Nanoengineering Heterogeneous Catalysts by Atomic Layer Deposition. *Annu. Rev. Chem. Biomol. Eng.* **2017**, *8*, 41−62.
(21) Pagán-Torres, Y. J.; Lu, J.; Nikolla, E.; Alba-Rubio, A. C. Well-Defined Nanostructures for Catalysis by Atomic Layer Deposition. *Stud. Surf. Sci. Catal.* **2017**, *177*, 643−676.
(22) O'Neill, B. J.; Jackson, D. H. K.; Crisci, A. J.; Farberow, C. A.; Shi, F.; Alba-Rubio, A. C.; Lu, J.; Dietrich, P. J.; Gu, X.; Marshall, C. L.; Stair, P. C.; Elam, J. W.; Miller, J. T.; Ribeiro, F. H.; Voyles, P. M.; Greeley, J.; Mavrikakis, M.; Scott, S. L.; Kuech, T. F.; Dumesic, J. A. Stabilization of Copper Catalysts for Liquid-Phase Reactions by Atomic Layer Deposition. *Angew. Chem., Int. Ed.* **2013**, *52*, 13808−13812.
(23) Yi, H.; Du, H.; Hu, Y.; Yan, H.; Jiang, H.-L.; Lu, J. Precisely Controlled Porous Alumina Overcoating on Pd Catalyst by Atomic Layer Deposition: Enhanced Selectivity and Durability in Hydrogenation of 1,3-Butadiene. *ACS Catal.* **2015**, *5*, 2735−2739.
(24) Gao, Z.; Qin, Y. Design and Properties of Confined Nanocatalysts by Atomic Layer Deposition. *Acc. Chem. Res.* **2017**, *50*, 2309−2316.
(25) Wang, C.; Hu, L.; Lin, Y.; Poeppelmeier, K.; Stair, P.; Marks, L. Controllable ALD Synthesis of Platinum Nanoparticles by Tuning Different Synthesis Parameters. *J. Phys. D: Appl. Phys.* **2017**, *50*, 415301.
(26) Mahurin, S.; Bao, L.; Yan, W.; Liang, C.; Dai, S. Atomic Layer Deposition of TiO_2 on Mesoporous Silica. *J. Non-Cryst. Solids* **2006**, *352*, 3280−3284.
(27) Zemtsova, E. G.; Arbenin, A. Y.; Plotnikov, A. F.; Smirnov, V. M. Pore Radius Fine Tuning of a Silica Matrix (MCM-41) Based on the Synthesis of Alumina Nanolayers with Different Thicknesses by Atomic Layer Deposition. *J. Vac. Sci. Technol., A* **2015**, *33*, 021519.
(28) Onn, T. M.; Küngas, R.; Fornasiero, P.; Huang, K.; Gorte, R. J. Atomic Layer Deposition on Porous Materials: Problems with Conventional Approaches to Catalyst and Fuel Cell Electrode Preparation. *Inorganics* **2018**, *6*, 34.
(29) Gallezot, P.; Richard, D. Selective Hydrogenation of α,β-Unsaturated Aldehydes. *Catal. Rev.: Sci. Eng.* **1998**, *40*, 81−126.
(30) Mäki-Arvela, P.; Hájek, J.; Salmi, T.; Murzin, D. Y. Chemoselective Hydrogenation of Carbonyl Compounds over Heterogeneous Catalysts. *Appl. Catal., A* **2005**, *292*, 1−49.
(31) Ji, X.; Niu, X.; Li, B.; Han, Q.; Yuan, F.; Zaera, F.; Zhu, Y.; Fu, H. Selective Hydrogenation of Cinnamaldehyde to Cinnamal Alcohol over Platinum/Graphene Catalysts. *ChemCatChem* **2014**, *6*, 3246−3253.
(32) Vannice, M. A.; Sen, B. Metal-Support Effects on the Intramolecular Selectivity of Crotonaldehyde Hydrogenation over Platinum. *J. Catal.* **1989**, *115*, 65−78.
(33) Englisch, M.; Jentys, A.; Lercher, J. A. Structure Sensitivity of the Hydrogenation of Crotonaldehyde over Pt/SiO_2 and Pt/TiO_2. *J. Catal.* **1997**, *166*, 25−35.
(34) Hidalgo-Carrillo, J.; Aramendía, M. A.; Marinas, A.; Marinas, J. M.; Urbano, F. J. Support and Solvent Effects on the Liquid-Phase Chemoselective Hydrogenation of Crotonaldehyde over Pt Catalysts. *Appl. Catal., A* **2010**, *385*, 190−200.
(35) Yang, X.; Mueanngern, Y.; Baker, Q. A.; Baker, L. R. Crotonaldehyde Hydrogenation on Platinum-Titanium Oxide and Platinum-Cerium Oxide Catalysts: Selective C═O Bond Hydrogen Requires Platinum Sites Beyond the Oxide-Metal Interface. *Catal. Sci. Technol.* **2016**, *6*, 6824−6835.
(36) Lu, J.; Kosuda, K. M.; Van Duyne, R. P.; Stair, P. C. Surface Acidity and Properties of TiO_2/SiO_2 Catalysts Prepared by Atomic Layer Deposition: UV−Visible Diffuse Reflectance, Drifts, and Visible Raman Spectroscopy Studies. *J. Phys. Chem. C* **2009**, *113*, 12412−12418.
(37) Jackson, D. H. K.; O'Neill, B. J.; Lee, J.; Huber, G. W.; Dumesic, J. A.; Kuech, T. F. Tuning Acid−Base Properties Using Mg−Al Oxide Atomic Layer Deposition. *ACS Appl. Mater. Interfaces* **2015**, *7*, 16573−16580.
(38) Hatton, B.; Kitaev, V.; Perovic, D.; Ozin, G.; Aizenberg, J. Low-Temperature Synthesis of Nanoscale Silica Multilayers - Atomic Layer Deposition in a Test Tube. *J. Mater. Chem.* **2010**, *20*, 6009−6013.
(39) Weng, Z.; Chen, Z.-h.; Qin, X.; Zaera, F. Sub-Monolayer Control of the Growth of Oxide Films on Mesoporous Materials. *J. Mater. Chem.* **2018**, Submitted.
(40) Ferguson, J. D.; Smith, E. R.; Weimer, A. W.; George, S. M. ALD of SiO_2 at Room Temperature Using Teos and H_2O with NH_3 as the Catalyst. *J. Electrochem. Soc.* **2004**, *151*, G528−G535.
(41) Tiznado, H.; Fuentes, S.; Zaera, F. Infrared Study of CO Adsorbed on Pd/Al_2O_3-ZrO_2. Effect of Zirconia Added by Impregnation. *Langmuir* **2004**, *20*, 10490−10497.
(42) Li, Y.; Zaera, F. Sensitivity of the Glycerol Oxidation Reaction to the Size and Shape of the Platinum Nanoparticles in Pt/SiO_2 Catalysts. *J. Catal.* **2015**, *326*, 116−126.
(43) Zhu, Y.; Zaera, F. Selectivity in the Catalytic Hydrogenation of Cinnamaldehyde Promoted by Pt/SiO_2 as a Function of Metal Nanoparticle Size. *Catal. Sci. Technol.* **2014**, *4*, 955−962.
(44) Zaera, F. Infrared Absorption Spectroscopy of Adsorbed CO: New Applications in Nanocatalysis for an Old Approach. *ChemCatChem* **2012**, *4*, 1525−1533.
(45) Feng, H.; Lu, J.; Stair, P.; Elam, J. Alumina over-Coating on Pd Nanoparticle Catalysts by Atomic Layer Deposition: Enhanced Stability and Reactivity. *Catal. Lett.* **2011**, *141*, 512−517.
(46) Lu, J.; Fu, B.; Kung, M. C.; Xiao, G.; Elam, J. W.; Kung, H. H.; Stair, P. C. Coking- and Sintering-Resistant Palladium Catalysts Achieved through Atomic Layer Deposition. *Science* **2012**, *335*, 1205−1208.
(47) Serrano-Ruiz, J. C.; López-Cudero, A.; Solla-Gullón, J.; Sepúlveda-Escribano, A.; Aldaz, A.; Rodríguez-Reinoso, F. Hydrogenation of α, β Unsaturated Aldehydes over Polycrystalline, (111) and (100) Preferentially Oriented Pt Nanoparticles Supported on Carbon. *J. Catal.* **2008**, *253*, 159−166.
(48) Zaki, M. I.; Hasan, M. A.; Al-Sagheer, F. A.; Pasupulety, L. In Situ FTIR Spectra of Pyridine Adsorbed on SiO_2−Al_2O_3, TiO_2, ZrO_2 and CeO_2: General Considerations for the Identification of Acid Sites on Surfaces of Finely Divided Metal Oxides. *Colloids Surf., A* **2001**, *190*, 261−274.
(49) Derouane, E. G.; Védrine, J. C.; Pinto, R. R.; Borges, P. M.; Costa, L.; Lemos, M. A. N. D. A.; Lemos, F.; Ribeiro, F. R. The Acidity of Zeolites: Concepts, Measurements and Relation to Catalysis: A Review on Experimental and Theoretical Methods for the Study of Zeolite Acidity. *Catal. Rev.: Sci. Eng.* **2013**, *55*, 454−515.
(50) Phung, T. K.; Lagazzo, A.; Rivero Crespo, M. Á.; Sánchez Escribano, V.; Busca, G. A Study of Commercial Transition Aluminas and of Their Catalytic Activity in the Dehydration of Ethanol. *J. Catal.* **2014**, *311*, 102−113.
(51) Parry, E. P. An Infrared Study of Pyridine Adsorbed on Acidic Solids. Characterization of Surface Acidity. *J. Catal.* **1963**, *2*, 371−379.
(52) Hughes, T. R.; White, H. M. A Study of the Surface Structure of Decationized Y Zeolite by Quantitative Infrared Spectroscopy. *J. Phys. Chem.* **1967**, *71*, 2192−2201.

DOI: 10.1021/acscatal.8b02431
ACS Catal. 2018, 8, 8513−8524

(53) Liu, X. Drifts Study of Surface of Γ-Alumina and Its Dehydroxylation. *J. Phys. Chem. C* **2008**, *112*, 5066−5073.
(54) Matsunaga, Y.; Yamazaki, H.; Yokoi, T.; Tatsumi, T.; Kondo, J. N. IR Characterization of Homogeneously Mixed Silica−Alumina Samples and Dealuminated Y Zeolites by Using Pyridine, CO, and Propene Probe Molecules. *J. Phys. Chem. C* **2013**, *117*, 14043−14050.
(55) Mouat, A. R.; George, C.; Kobayashi, T.; Pruski, M.; van Duyne, R. P.; Marks, T. J.; Stair, P. C. Highly Dispersed SiO_x/Al_2O_3 Catalysts Illuminate the Reactivity of Isolated Silanol Sites. *Angew. Chem., Int. Ed.* **2015**, *54*, 13346−13351.
(56) Ardagh, M. A.; Bo, Z.; Nauert, S. L.; Notestein, J. M. Depositing SiO_2 on Al_2O_3: A Route to Tunable Brønsted Acid Catalysts. *ACS Catal.* **2016**, *6*, 6156−6164.
(57) Arai, M.; Usui, K.-i.; Nishiyama, Y. Preparation of Alumina-Supported Platinum Catalyst at Ambient Temperature for Selective Synthesis of Cinnamyl Alcohol by Liquid-Phase Cinnamaldehyde Hydrogenation. *J. Chem. Soc., Chem. Commun.* **1993**, 1853−1854.
(58) Arai, M.; Obata, A.; Usui, K.; Shirai, M.; Nishiyama, Y. Activity for Liquid-Phase Hydrogenation of α,β-Unsaturated Aldehydes of Supported Platinum Catalysts Prepared through Low-Temperature Reduction. *Appl. Catal., A* **1996**, *146*, 381−389.
(59) Yuan, Y.; Yao, S.; Wang, M.; Lou, S.; Yan, N. Recent Progress in Chemoselective Hydrogenation of α,β-Unsaturated Aldehyde to Unsaturated Alcohol over Nanomaterials. *Curr. Org. Chem.* **2013**, *17*, 400−413.
(60) Kahsar, K. R.; Schwartz, D. K.; Medlin, J. W. Control of Metal Catalyst Selectivity through Specific Noncovalent Molecular Interactions. *J. Am. Chem. Soc.* **2014**, *136*, 520−526.
(61) Weng, Z.; Zaera, F. Increase in Activity and Selectivity in Catalysis via Surface Modification with Self-Assembled Monolayers. *J. Phys. Chem. C* **2014**, *118*, 3672−3679.
(62) Pang, S. H.; Medlin, J. W. Controlling Catalytic Selectivity via Adsorbate Orientation on the Surface: From Furfural Deoxygenation to Reactions of Epoxides. *J. Phys. Chem. Lett.* **2015**, *6*, 1348−1356.
(63) Coloma, F.; Llorca, J.; Homs, N.; Ramirez de la Piscina, P.; Rodriguez-Reinoso, F.; Sepulveda-Escribano, A. Crotonaldehyde Hydrogenation over Alumina- and Silica-Supported Pt-Sn Catalysts of Different Composition. In Situ DRIFT Study. *Phys. Chem. Chem. Phys.* **2000**, *2*, 3063−3069.
(64) Dong, Y.; Zaera, F. Selectivity in Hydrogenation Catalysis with Unsaturated Aldehydes: Parallel Versus Sequential Steps. *J. Phys. Chem. Lett.* **2018**, *9*, 1301−1306.
(65) Giroir-Fendler, A.; Richard, D.; Gallezot, P. Chemioselectivity in the Catalytic Hydrogenation of Cinnamaldehyde. Effect of Metal Particle Morphology. *Catal. Lett.* **1990**, *5*, 175−182.
(66) Plomp, A. J.; Vuori, H.; Krause, A. O. I.; de Jong, K. P.; Bitter, J. H. Particle Size Effects for Carbon Nanofiber Supported Platinum and Ruthenium Catalysts for the Selective Hydrogenation of Cinnamaldehyde. *Appl. Catal., A* **2008**, *351*, 9−15.
(67) Busca, G. Acid Catalysts in Industrial Hydrocarbon Chemistry. *Chem. Rev.* **2007**, *107*, 5366−5410.
(68) Vjunov, A.; Fulton, J. L.; Huthwelker, T.; Pin, S.; Mei, D.; Schenter, G. K.; Govind, N.; Camaioni, D. M.; Hu, J. Z.; Lercher, J. A. Quantitatively Probing the Al Distribution in Zeolites. *J. Am. Chem. Soc.* **2014**, *136*, 8296−8306.
(69) Caillot, M.; Chaumonnot, A.; Digne, M.; van Bokhoven, J. A. The Variety of Brønsted Acid Sites in Amorphous Aluminosilicates and Zeolites. *J. Catal.* **2014**, *316*, 47−56.
(70) Martínez, C.; Corma, A. Inorganic Molecular Sieves: Preparation, Modification and Industrial Application in Catalytic Processes. *Coord. Chem. Rev.* **2011**, *255*, 1558−1580.
(71) Armor, J. N. A History of Industrial Catalysis. *Catal. Today* **2011**, *163*, 3−9.
(72) Hensen, E. J. M.; Poduval, D. G.; Magusin, P. C. M. M.; Coumans, A. E.; van Veen, J. A. R. Formation of Acid Sites in Amorphous Silica-Alumina. *J. Catal.* **2010**, *269*, 201−218.
(73) Leydier, F.; Chizallet, C.; Chaumonnot, A.; Digne, M.; Soyer, E.; Quoineaud, A.-A.; Costa, D.; Raybaud, P. Brønsted Acidity of Amorphous Silica−Alumina: The Molecular Rules of Proton Transfer. *J. Catal.* **2011**, *284*, 215−229.
(74) Valla, M.; Rossini, A. J.; Caillot, M.; Chizallet, C.; Raybaud, P.; Digne, M.; Chaumonnot, A.; Lesage, A.; Emsley, L.; van Bokhoven, J. A.; Copéret, C. Atomic Description of the Interface between Silica and Alumina in Aluminosilicates through Dynamic Nuclear Polarization Surface-Enhanced NMR Spectroscopy and First-Principles Calculations. *J. Am. Chem. Soc.* **2015**, *137*, 10710−10719.
(75) Hansford, R. C. Mechanism of Catalytic Cracking. *Ind. Eng. Chem.* **1947**, *39*, 849−852.
(76) Thomas, C. L. Chemistry of Cracking Catalysts. *Ind. Eng. Chem.* **1949**, *41*, 2564−2573.
(77) Tamele, M. W. Chemistry of the Surface and the Activity of Alumina-Silica Cracking Catalyst. *Discuss. Faraday Soc.* **1950**, *8*, 270−279.
(78) Xu, B.; Sievers, C.; Lercher, J. A.; van Veen, J. A. R.; Giltay, P.; Prins, R.; van Bokhoven, J. A. Strong Brønsted Acidity in Amorphous Silica−Aluminas. *J. Phys. Chem. C* **2007**, *111*, 12075−12079.
(79) Poduval, D. G.; van Veen, J. A. R.; Rigutto, M. S.; Hensen, E. J. M. Bronsted Acid Sites of Zeolitic Strength in Amorphous Silica-Alumina. *Chem. Commun.* **2010**, *46*, 3466−3468.
(80) Hensen, E. J. M.; Poduval, D. G.; Degirmenci, V.; Ligthart, D. A. J. M.; Chen, W.; Maugé, F.; Rigutto, M. S.; van Veen, J. A. R. Acidity Characterization of Amorphous Silica−Alumina. *J. Phys. Chem. C* **2012**, *116*, 21416−21429.
(81) Crépeau, G.; Montouillout, V.; Vimont, A.; Mariey, L.; Cseri, T.; Maugé, F. Nature, Structure and Strength of the Acidic Sites of Amorphous Silica Alumina: An IR and NMR Study. *J. Phys. Chem. B* **2006**, *110*, 15172−15185.
(82) Huang, J.; van Vegten, N.; Jiang, Y.; Hunger, M.; Baiker, A. Increasing the Brønsted Acidity of Flame-Derived Silica/Alumina up to Zeolitic Strength. *Angew. Chem., Int. Ed.* **2010**, *49*, 7776−7781.
(83) Caillot, M.; Chaumonnot, A.; Digne, M.; Bokhoven, J. A. V. Quantification of Brønsted Acid Sites of Grafted Amorphous Silica−Alumina Compounds and Their Turnover Frequency in m-Xylene Isomerization. *ChemCatChem* **2013**, *5*, 3644−3656.
(84) Caillot, M.; Chaumonnot, A.; Digne, M.; Poleunis, C.; Debecker, D. P.; van Bokhoven, J. A. Synthesis of Amorphous Aluminosilicates by Grafting: Tuning the Building and Final Structure of the Deposit by Selecting the Appropriate Synthesis Conditions. *Microporous Mesoporous Mater.* **2014**, *185*, 179−189.
(85) Yang, N.; Bent, S. F. Investigation of Inherent Differences between Oxide Supports in Heterogeneous Catalysis in the Absence of Structural Variations. *J. Catal.* **2017**, *351*, 49−58.
(86) Gates, B. C.; Katzer, J. R.; Schuit, G. C. A. *Chemistry of Catalytic Processes*; McGraw-Hill: New York, 1979.
(87) Szöllösi, G.; Török, B.; Szakonyi, G.; Kun, I.; Bartók, M. Ultrasonic Irradiation as Activity and Selectivity Improving Factor in the Hydrogenation of Cinnamaldehyde over Pt/SiO_2 Catalysts. *Appl. Catal., A* **1998**, *172*, 225−232.
(88) Lashdaf, M.; Lahtinen, J.; Lindblad, M.; Venäläinen, T.; Krause, A. O. I. Platinum Catalysts on Alumina and Silica Prepared by Gas- and Liquid- Phase Deposition in Cinnamaldehyde Hydrogenation. *Appl. Catal., A* **2004**, *276*, 129−137.
(89) Stolle, A.; Gallert, T.; Schmoger, C.; Ondruschka, B. Hydrogenation of Citral: A Wide-Spread Model Reaction for Selective Reduction of α,β-Unsaturated Aldehydes. *RSC Adv.* **2013**, *3*, 2112−2153.
(90) Kašpar, J.; Graziani, M.; Escobar, G. P.; Trovarelli, A. Chemoselective Hydrogenation of Unsaturated Carbonyl Compounds over Groups 8 and 9 Titania-Supported Metal Catalysts. *J. Mol. Catal.* **1992**, *72*, 243−251.
(91) Boutonnet Kizling, M.; Bigey, C.; Touroude, R. Novel Method of Catalyst Preparation for Selective Hydrogenation of Unsaturated Aldehydes. *Appl. Catal., A* **1996**, *135*, L13−L17.
(92) Claus, P. Selective Hydrogenation of α,β-Unsaturated Aldehydes and Other C═O and C═C Bonds Containing Compounds. *Top. Catal.* **1998**, *5*, 51−62.

DOI: 10.1021/acscatal.8b02431
ACS Catal. 2018, 8, 8513−8524

(93) Abid, M.; Paul-Boncour, V.; Touroude, R. Pt/CeO_2 Catalysts in Crotonaldehyde Hydrogenation: Selectivity, Metal Particle Size and SMSI States. *Appl. Catal., A* **2006**, *297*, 48−59.
(94) Chiu, T.-C.; Lee, H.-Y.; Li, P.-H.; Chao, J.-H.; Lin, C.-H. Effects of Interfacial Charge and the Particle Size of Titanate Nanotube-Supported Pt Nanoparticles on the Hydrogenation of Cinnamaldehyde. *Nanotechnology* **2013**, *24*, 115601.
(95) Delbecq, F.; Li, Y.; Loffreda, D. Metal−Support Interaction Effects on Chemo−Regioselectivity: Hydrogenation of Crotonaldehyde on $Pt_{13}/CeO_2(111)$. *J. Catal.* **2016**, *334*, 68−78.
(96) Kennedy, R. M.; Crosby, L. A.; Ding, K.; Canlas, C. P.; Gulec, A.; Marks, L. D.; Elam, J. W.; Marshall, C. L.; Poeppelmeier, K. R.; Stair, P. C. Replication of SMSI via ALD: TiO_2 Overcoats Increase Pt-Catalyzed Acrolein Hydrogenation Selectivity. *Catal. Lett.* **2018**, *148*, 2223−2232.
(97) Loffreda, D.; Delbecq, F.; Vigné, F.; Sautet, P. Fast Prediction of Selectivity in Heterogeneous Catalysis from Extended Brønsted-Evans-Polanyi Relations: A Theoretical Insight. *Angew. Chem., Int. Ed.* **2009**, *48*, 8978−8980.
(98) Zaera, F. The Surface Chemistry of Metal-Based Hydrogenation Catalysis. *ACS Catal.* **2017**, *7*, 4947−4967.
(99) Zaera, F. Key Unanswered Questions About the Mechanism of Olefin Hydrogenation Catalysis by Transition-Metal Surfaces: A Surface-Science Perspective. *Phys. Chem. Chem. Phys.* **2013**, *15*, 11988−12003.
(100) Zaera, F. Outstanding Mechanistic Questions in Heterogeneous Catalysis. *J. Phys. Chem. B* **2002**, *106*, 4043−4052.
(101) Somorjai, G.; Kliewer, C. Reaction Selectivity in Heterogeneous Catalysis: An Invited Review. *React. Kinet. Catal. Lett.* **2009**, *96*, 191−208.
(102) Zaera, F. Regio, Stereo, and Enantio Selectivity in Hydrocarbon Conversion on Metal Surfaces. *Acc. Chem. Res.* **2009**, *42*, 1152−1160.

DOI: 10.1021/acscatal.8b02431
ACS Catal. 2018, 8, 8513−8524